

1 Exploring foraminiferal Sr/Ca as a new carbonate system proxy

2  
3 Nina Keul<sup>1</sup> (corresponding author), Gerald Langer<sup>2</sup>, Silke Thoms<sup>3</sup>, Lennart Jan de Nooijer<sup>4</sup>,  
4 Gert-Jan Reichart<sup>4,5</sup>, Jelle Bijma<sup>3</sup>

5  
6 <sup>1</sup> Marine Geosciences, Kiel University, Germany (nina.keul@gmail.com)

7 <sup>2</sup> The Marine Biological Association of the United Kingdom, The Laboratory, Citadel Hill,  
8 Plymouth, Devon, PL1 2PB, UK

9 <sup>3</sup> Biogeosciences, Alfred-Wegener-Institut Helmholtz-Zentrum für Polar und  
10 Meeresforschung, Bremerhaven, Germany

11 <sup>4</sup> Dept. of Geology and Chemical Oceanography, Royal Netherlands Institute for Sea  
12 Research (NIOZ) and Utrecht University, Landsdiep 4, 1797 SZ 't Horntje (Texel), The  
13 Netherlands

14 <sup>5</sup> Dept. of Earth Sciences, Utrecht University, Budapestlaan 4, 3584 CD Utrecht, The  
15 Netherlands.

16  
17 abstract

18 In present day paleoclimate research one of the most pressing challenges is the reconstruction  
19 of atmospheric CO<sub>2</sub> concentrations. A variety of proxies for several components of the  
20 marine inorganic carbon system have been developed in this context (e.g. B isotopes, B/Ca,  
21 U/Ca) to allow reconstruction of past seawater pH, alkalinity etc., and thereby facilitate  
22 estimates of past atmospheric pCO<sub>2</sub>. Based on culture experiments using the benthic  
23 foraminifera *Ammonia sp.* we describe a positive correlation between Sr/Ca and the carbonate  
24 system, namely DIC/ bicarbonate ion concentration. Foraminiferal Sr/Ca ratios provide  
25 potentially additional constraints on the carbonate system proxy, because the analysis of  
26 foraminiferal carbonate Sr/Ca is straightforward and not easily contaminated. Applying our  
27 calibration to a published dataset of paleo-Sr/Ca suggests the validity of Sr/Ca as a carbonate  
28 system proxy. Furthermore, we explore how our data can be used to advance conceptual  
29 understanding of the foraminiferal biomineralization mechanism.

30  
31 1. Introduction

32 Incorporation of elements dissolved in seawater (e.g. Na, Mg, Sr, B) into biogenic calcium  
33 carbonate during calcification is influenced by a combination of various environmental  
34 parameters and biological processes. Element to calcium ratios in the calcium carbonate of  
35 calcifying organisms, such as foraminifera and corals, are therefore used to reconstruct past  
36 oceanographic conditions (Boyle, 1988; Delaney et al., 1985; Emiliani, 1955). The Mg/Ca  
37 ratio of foraminiferal tests, for instance, is a relatively established reconstruction tool for past  
38 seawater temperatures (Nürnberg et al., 1996). Due to ongoing anthropogenic CO<sub>2</sub> emissions  
39 and concomitant acidification of sea surface waters (i.e. ocean acidification) studying past  
40 changes in seawater carbonate chemistry has become a major focus in paleoclimate research  
41 (e.g. Hönisch et al., 2012; Bijma et al., 2013). Particularly rapid acidification events in the  
42 geological past such as associated with the PETM (Paleocene–Eocene Thermal Maximum)  
43 might provide important constraints for forecasting shifts in ecosystem and or community  
44 composition during such transitions (Kiessling and Simpson, 2011; Rodríguez-Tovar et al.,  
45 2011). Insight into (long-term) marine carbon cycling and perturbations therein critically  
46 depend on robust reconstruction of at least two parameters of the seawater carbonate system  
47 (Zeebe and Wolf-Gladrow, 2001).

48 For reconstructing past seawater carbonate chemistry, foraminiferal test boron content and  
49 their stable isotope ratios are, for example, used (Hemming and Hanson, 1992; Hönisch et  
50 al., 2009; Sanyal et al., 1995, 1999, 2000, 2001; Yu et al., 2007, 2010). Still, accurate  
51 determination of B/Ca and  $\delta^{11}\text{B}$  remains challenging and the uptake of boron and its  
52 consequent incorporation and or speciation are not fully understood on a process level  
53 (Kaczmarek et al., 2015). Other C-system (carbonate system) proxies include for instance the  
54 Cd/Ca and Zn/Ca ratios in benthic foraminifera, since they correlate with the relative level of  
55 oversaturation ( $\Delta\text{CO}_3^{2-}$ ; Marchitto et al., 2000; 2002). Planktonic (Bijma et al., 2002;  
56 Broecker and Clark, 2002) and benthic (Keul et al., 2013a) foraminiferal test weight  
57 normalized to size has been shown to correlate with seawater carbonate ion concentration.  
58 Furthermore, it has been shown that foraminiferal U/Ca variability reflects changes in carbon  
59 speciation (Keul et al., 2013b; Raitzsch et al., 2011; Russell et al., 2004).

60  
61 Of the different elements that are analyzed in carbonate, Sr is analytically one of the most  
62 robust, with high accuracy and precision. Values for Sr/Ca are hence relatively well-studied  
63 and have been related to different processes in a variety of organisms, such as temperature in  
64 corals (Smith and Roth, 1979), calcification- and growth-rates in coccolithophorids (Stoll and  
65 Schrag, 2000, 2001) and has been shown to be influenced by growth rates, temperature,  
66 salinity and pH in foraminifera (Kisakürek et al., 2008; Lea et al., 1999). Foraminiferal Sr/Ca  
67 has been shown to vary with water depth (e.g. McCorkle et al., 1995; Elderfield et al., 1996,  
68 Lear et al., 2003; Rosenthal et al., 2006; Yu et al. 2014), which could be caused by  
69 parameters changing with depth, such as pressure, temperature (e.g. Rosenthal et al., 1997)  
70 and/ or carbonate ion concentration. It has been shown in many studies that foraminiferal  
71 Sr/Ca varies with seawater carbonate chemistry (e.g. Dissard et al., 2010; Dueñas-Bohórquez  
72 et al., 2009, 2011; Lea et al., 1999; Raitzsch et al., 2010; Russell et al., 2004). The effect  
73 seems to be species specific, because three planktonic species (*Globigerinoides sacculifer*,  
74 *Globigerina bulloides*, *Orbulina universa*) show an increase in Sr/Ca with increasing pH,  
75 whereas no response was observed for a benthic species (*Heterostegina depressa*) and  
76 another planktonic species (*Globigerinoides ruber*). For the benthic species *Ammonia sp.*, the  
77 response of Sr-incorporation to changing carbonate chemistry is ambiguous: while Dueñas-  
78 Bohórquez et al. (2009) observed no impact of changing carbonate chemistry, Dissard and  
79 colleagues (2010) found a distinct increase in Sr incorporation with increasing pH. Hence,  
80 whereas Sr/Ca is obviously sensitive to environmental parameters, response to these  
81 parameters is not univocal.

82  
83 Compared to reconstructing temperature (based on e.g. foraminiferal Mg/Ca and  $\delta^{18}\text{O}$ ),  
84 proxies for C-system parameters are generally less robust and reconstructions based thereon  
85 are thus susceptible to a number of uncertainties (Pagani et al., 2005). The source of  
86 uncertainty of C-system proxies stems, to a considerable extent, from the fact that the  
87 seawater C-system consists of six inter-correlated parameters (Zeebe and Wolf-Gladrow,  
88 2001). This inter-correlation usually renders the identification of a single parameter causing  
89 changes to, e.g., B/Ca impossible. The only way to resolve this inter-relation is by  
90 experimentally deconvolving the impact of different C-system parameters on foraminiferal  
91 carbonate chemistry proxies (e.g. Kaczmarek et al., 2015, Keul et al., 2013b). Almost all  
92 experimental studies dealing with the C-system employed either a TA (total alkalinity) or a  
93 DIC (dissolved inorganic carbon) manipulation (also termed classical C-system  
94 manipulations). In both cases changes in, e.g., pH and carbonate ion concentration are

95 correlated, so that an observed effect cannot be traced back to an individual parameter such as  
96 pH or carbonate ion concentration. The latter information is crucial for a process based  
97 understanding of the potential impact of carbonate chemistry on Sr/Ca. In this context,  
98 especially the uptake mechanism of divalent ions is of interest. Several conceptual  
99 biomineralization models have been proposed for foraminifera (see de Nooijer et al., 2014b  
100 for an overview). It has long been recognized that foraminifera exert a tight control on their  
101 calcification process (Röttger, 1973; Spindler and Röttger, 1973; Hemleben et al., 1989). This  
102 is accomplished by precipitating calcite in a confined space (the so-called site of calcification,  
103 SOC or delimited biomineralization space, DBS). The DBS represents no significant ion-  
104 reservoir for chamber formation and therefore requires constant supply of Ca and DIC, which  
105 was originally assumed to be delivered by vesicles (Bentov and Erez, 2006; Erez, 2003). The  
106 exclusive transport of Ca by vesicles, however, makes it difficult to account for element  
107 partitioning. Therefore, an alternative ion transport model, although including vesicle  
108 transport, centrally features transmembrane ion transport (Glas et al., 2012; Keul et al.,  
109 2013b; Mewes et al., 2014; Nehrke et al., 2013). During trans-membrane Ca uptake, Sr is  
110 accidentally taken up because calcium transport proteins also admit other ions to a certain  
111 extent, especially Sr and Ba (Berman and King, 1990). Since transmembrane transport is  
112 tightly regulated by all eukaryotic cells, such an ion transport model explains the fine-tuned  
113 control on all relevant parameters concerning calcite precipitation.

114

115 In this study we use a non-classical, i.e. combined TA/DIC, manipulation of the C-system in  
116 order to identify parameters of the C-system affecting test Sr/Ca in the benthic foraminifer  
117 *Ammonia sp.* ("Ammonia molecular type T6", Hayward et al., 2004). The Sr/Ca-C-system  
118 relationship is subsequently applied to a published dataset of paleo-Sr/Ca to explore the  
119 validity of Sr/Ca as a C-system proxy in different species. We also present a calcification  
120 model which demonstrates that the effect of seawater carbonate chemistry on Sr partitioning  
121 is in line with current understanding of minor element partitioning in foraminifera.

122

## 123 2. Material & Methods

### 124 2.1. Sample Collection and Culturing

125 Surface sediments of intertidal mudflats of the Wadden Sea near Dorum, Germany, were  
126 sampled for foraminifera between January and March 2011. The macrofauna was removed  
127 upon return at the laboratory by sieving over a 1 mm-screen. Sieved sediments were  
128 transferred to aquariums, submerged in 0.2  $\mu\text{m}$  filtered North Sea water (S=33, pH=8.1) and  
129 stored at 10°C. Prior to the culture experiments, living adult specimens of *Ammonia sp.* were  
130 isolated from these sediments and transferred to well plates at 25°C and fed every second day  
131 *Dunaliella salina*. After about one week ca. 10% of the adult specimen had reproduced  
132 asexually, yielding between 50 and 200 juveniles per reproduction event (De Nooijer et al.,  
133 2014a). After 2-3 days, these juveniles had built 3-4 chambers and were transferred into the  
134 culture experiments.

135

### 136 2.2. Seawater preparations

137 A total of eight culture media were prepared using sterile-filtered (0.2  $\mu\text{m}$  pore size) North  
138 Sea water (see Keul et al., 2013b for details). Borosilicate flasks containing the manipulated  
139 seawater were sealed headspace-free and gas-tight with Teflon-lined caps and kept at 3°C  
140 until use in the experiments. The eight treatments were divided into two groups using two  
141 different C-system perturbations (Tab. 1):

142  
143  
144  
145  
146  
147  
148  
149  
150  
151  
152  
153  
154  
155  
156  
157  
158  
159  
160  
161  
162  
163  
164  
165  
166  
167  
168  
169  
170  
171  
172  
173  
174  
175  
176  
177  
178  
179  
180  
181  
182  
183  
184  
185  
186  
187  
188

a) "TA manipulation": four treatments, covering a range of  $[\text{CO}_3^{2-}]$  and pHs, while DIC remained constant.

b) "pH-stable manipulation": four seawater manipulations, where DIC and TA were manipulated as to keep pH constant, the corresponding  $p\text{CO}_2$  values were matched to those of the TA-manipulation.

### 2.3. Experimental Setup and Culturing

The duration of the culture experiments was between 59 and 96 days, requiring an experimental setup that allowed maintaining the C-system parameters constant for this period. The experimental setup (see Keul et al., 2013b for details) consisted of four gas-tight boxes, through which air with four different  $\text{CO}_2$  concentrations (Tab. 1) was purged. Juvenile foraminifera were placed into Petri dishes containing manipulated seawater, long-term stability was ensured by matching the  $\text{CO}_2(\text{aq})$  of the manipulated culture media to the  $p\text{CO}_2$  in the gas-tight boxes. The complete setup was placed in a temperature-controlled room ( $26^\circ\text{C}$ ) with a natural day to night light cycle (12h/12h). Water in the Petri dishes was exchanged every two to three days. To ensure pre-equilibration of the borosilicate bottles containing the manipulated seawater, they were unsealed and stored in the boxes prior to water-exchange. After water exchange, foraminifera were fed heat-sterilized algae (*D. salina*). Petri dishes were exchanged every two weeks to minimize bacterial growth on the bottom of the dishes due to accumulation of waste material. Foraminifera were harvested at the end of the culture period, the organics removed with  $\text{NaOCl}$ , rinsed thoroughly with ultrapure water and dried.

### 2.4. Sample analysis

#### 2.4.1. Carbonate chemistry

Acid-washed 13mL borosilicate flasks were filled headspace-free and kept at  $0^\circ\text{C}$  until measurement of DIC (within 3 days). DIC was measured photometrically in duplicates with a QuAAatro autoanalyzer (Seal Analytical, Meqon, USA). Repeated measurements of a batch of North Sea seawater sampled in surface waters off Helgoland (Germany) were carried out to determine the average precision, which was  $\pm 10 \mu\text{mol/kg-sw}$ . Batches of seawater sampled in the same location (off Helgoland) were used earlier to determine the precision of the DIC measurements (e.g. Langer et al. 2009). Batch No. 54 of A. Dicksons Certified Reference Material Seawater (Marine Physical Laboratory, Scripps Institution of Oceanography) was measured to account for inaccuracies in the measurements. The pH was measured potentiometrically using a two-point NBS-calibrated glass electrode (Schott Instruments, Mainz, Germany) interfaced to a WTW pH-meter. Conversion to total scale was achieved by the simultaneous measurements of a Tris seawater buffer (Tris/Tris-HCl buffer in artificial seawater, Dickson et al., 2007) and values reported here are on this scale. A conductivity meter (WTW Multi 340i) interfaced to a TetraCon 325 sensor was used to measure temperature and salinity. Input parameters DIC and pH (Hoppe et al., 2012) were used to calculate the C-system parameters using the CO2SYS program adapted to Excel by Pierrot et al., 2006. The equilibrium constants  $K_1$  and  $K_2$  were used of Mehrbach et al. (1973), as reformulated by Dickson and Millero (1987).

#### 189 2.4.2. Elemental concentration of culturing media

190 Inductively coupled plasma optical emission spectrometry (ICP-OES) was used to determine  
191 the strontium and calcium concentration of the eight manipulated seawater treatments.

192 Calcium ( $\text{Ca}^{2+}$ ) was measured at a wavelength of 316 nm, Strontium ( $\text{Sr}^{2+}$ ) at 408 nm (Table  
193 1), with a relative standard deviation <1%.

194

#### 195 2.4.3. Elemental composition of foraminiferal calcite

196 The LA-ICP-MS (laser ablation-inductively coupled plasma-mass spectrometry) system at  
197 Utrecht University (Reichert et al., 2003) was used to determine elemental concentrations of  
198 cleaned foraminiferal tests. It consists of a sector-field mass spectrometer (Element 2,  
199 Thermo Scientific) connected to an excimer laser (Lambda Physik), equipped with GeoLas  
200 200Q optics. The pulse repetition rate was set to 6 Hz, energy density was  $\sim 1 \text{ J cm}^{-2}$  and  
201 ablation beam diameter was set at 80  $\mu\text{m}$ . Counts of  $^{24}\text{Mg}$ ,  $^{27}\text{Al}$ ,  $^{43}\text{Ca}$ ,  $^{44}\text{Ca}$ ,  $^{55}\text{Mn}$ ,  $^{88}\text{Sr}$ ,  $^{238}\text{U}$   
202 were used to calculate elemental concentrations in the samples. A complete measurement  
203 cycle through all masses took 0.52 s. The ablation profiles were checked for potential surface  
204 contamination using  $^{27}\text{Al}$ . A NIST glass (SRM NIST 610) was ablated three times and an in-  
205 house matrix-matched calcite once between every 10 samples. Relative variability for this  
206 calcites Sr/Ca during measurements was <3 % (rsd), matching variability reported in Raitzsch  
207 et al. (2010). The NIST610 was ablated at a higher energy density ( $\sim 5 \text{ J cm}^{-2}$ ). Assuming 40  
208 weight % calcium in calcite,  $^{43}\text{Ca}$  was used as an internal standard, while counts for  $^{44}\text{Ca}$   
209 were used to check for consistency. Using the software package Glitter (software for data  
210 reduction, GEMOC; Van Achterbergh et al., 2001, Griffin et al., 2008), time resolved counts  
211 during ablation of the test were integrated and the background subtracted. Isotopic counts  
212 were standardized to  $^{43}\text{Ca}$  and converted to concentrations using the signals obtained on the  
213 NIST glass assuming standard natural isotopic abundances and values reported by Jochum et  
214 al. (2011).

215 Six individual specimens (seven in treatment A1) were analyzed per treatment and between  
216 five to seven individual laser spot measurements were obtained for each specimen, together  
217 equaling 276 single spot measurements. During the measurements, the laser protruded  
218 sequentially deeper parts of the test and measurements were stopped once the laser had  
219 protruded through the test. Five ablation profiles were discarded because the chamber walls  
220 were too thin and the resulting ablation profiles too short for reliable determination of  
221 element/Ca ratios. Using measured seawater Sr/Ca ratios, the empirical partition coefficient  
222 for strontium in foraminiferal calcite ( $D_{\text{Sr}}$ ) was calculated according to:

223

$$224 \quad D_{\text{Sr}} = \frac{\left(\frac{\text{Sr}}{\text{Ca}}\right)_{\text{CC}}}{\left(\frac{\text{Sr}}{\text{Ca}}\right)_{\text{SW}}} \quad (1)$$

225

226 where  $(\text{Sr}/\text{Ca})_{\text{CC}}$  refers to the measured molar ratio of Sr and Ca in foraminiferal calcite and  
227  $(\text{Sr}/\text{Ca})_{\text{SW}}$  to that in the culture media.

228 Variability in the foraminiferal Sr/Ca, as expressed by the relative standard deviation (rsd,  
229 defined as the ratio of the standard deviation ('sigma') to the mean, expressed in percent), was  
230 with 7.2-15.3% relatively low for LA-ICP-MS measurements on foraminifera, when  
231 compared to ICP-MS analyses of whole, acid-dissolved tests, where intratest inhomogeneity  
232 cannot be resolved. There was no detectable effect of the treatments on variability in obtained  
233 Sr/Ca. Average intratest variability (9.2% rsd) was lower than average intertest variability  
234 (15.3% rsd). Uncertainty in the measurements can arise from measuring too few single spots/

235 individuals. This can be expressed as standard error (defined as the ratio of the standard  
236 deviation to the square root of the sample size, here number of measurements) and is  
237 calculated from the *rsd*, with lower errors associated with increasing number of  
238 measurements. When measuring 5, 10, or 20 single spots per individual, the standard errors  
239 are 4, 3 and 2% respectively and when measuring 5, 10, or 20 individuals, the associated  
240 uncertainty is 3, 5 and 7%, respectively. Consequently, the 5-7 measurements per individual  
241 test entail an uncertainty of 3.5-4.1%, and the limitation to 6-7 individuals entails a standard  
242 error of 6.2-5.8%.

243  
244  
245

#### 246 2.4.4. Foraminiferal growth

247 Foraminiferal growth rates were determined from the final weight of dead specimens (Mettler  
248 Toledo UMX 2 Ultra Microbalance, 0.1  $\mu\text{g}$  precision), as described in (Keul et al., 2013a).  
249 Growth rates are defined as the mass of calcite grown per specimen per unit time ( $\mu\text{g}/\text{d}/\text{ind}$ ).  
250 It should be noted, that this refers to bulk growth rate. Instantaneous growth rate (e.g. during  
251 the intermittent addition of new chambers) cannot be assessed this way.

252  
253

#### 254 2.5. Statistics

255 The statistics environment R (R Development Core Team, 2012; <http://www.R-project.org>)  
256 was used for statistical analysis. Analysis of variance (ANOVA) was performed to determine  
257 the effect of the individual parameters of the C-system on foraminiferal Sr/Ca. Log  
258 transformation ensured normally distributed data (Shapiro test,  $p > 0.05$ ) and the null-  
259 hypothesis of the ANOVA (all group means are equal) was rejected at the 5% level ( $p < 0.05$ ).  
260 Average values and 2SE (standard errors) are reported throughout the text.

261  
262

### 263 3. Results

#### 264 3.1 Foraminiferal Sr/Ca and $D_{Sr}$

265 Average foraminiferal Sr/Ca values range from 1.1 to 1.7 mmol/mol, with individual spot  
266 measurements ranging from 0.85 to 2.20 mmol/mol. The range in the distribution coefficient  
267 for strontium,  $D_{Sr}$  (the ratio of Sr/Ca<sub>CC</sub> to Sr/Ca<sub>SW</sub>), has a similar magnitude in individual  
268 measurements and means: 0.13 to 0.37 for individual spot measurements, while mean  $D_{Sr}$   
269 ranges from 0.17 to 0.29. The highest strontium concentration was found in tests of  
270 individuals cultured in treatment B4, characterized by the highest  $pCO_2$  and highest DIC of  
271 the pH-stable treatment. The Sr/Ca and consequently  $D_{Sr}$  are relatively homogeneous in tests  
272 grown in the TA manipulation (A1-A4), whereas the range in Sr/Ca and  $D_{Sr}$  from individuals  
273 grown in the pH-stable manipulation is more variable (B1-B4, Fig. 1).

274

275

#### 276 3.2. Correlation between foraminiferal Sr/Ca and C-system

277 Single spot measurements from the same specimen were averaged and linear regression  
278 analyses were performed to analyze correlation between individual C-system parameters and  
279 foraminiferal Sr/Ca. Results of the regression analyses (intercept and slope) and the statistical  
280 output ( $p$ ,  $R^2$  and  $F$ ) are summarized in Tab. 2. All regressions were highly significant ( $p <$   
281 0.05) and explain, depending on the C-system parameter, between 23 and 64% of the  
282 observed variability in  $D_{Sr}$ . The corresponding plots of the regression analyses are shown in  
283 Fig. 1.

284

285

### 286 4. Discussion

#### 287 4.1. Sr incorporation in other foraminiferal species

288 Previous culturing studies on *Ammonia sp.* reported  $D_{Sr}$  values of 0.15-0.18 (Dissard et al.,  
289 2010), 0.16-0.17 (Raitzsch et al., 2010), 0.16-0.19 (Dueñas-Bohórquez et al., 2011), 0.16-  
290 0.20 (De Nooijer et al., 2014a), which is in good agreement with the range of mean  $D_{Sr}$  of  
291 0.19-0.20 determined on specimens from the TA-manipulation (Fig. 2, blue crosses). The  $D_{Sr}$   
292 values of the tests grown in the pH-stable manipulation (Fig. 2; 0.17-0.29) are higher and are  
293 higher and indicate that the C-system parameters primarily affecting foram  $D_{Sr}$  must be  
294 changing  $D_{Sr}$ , whereas it must be relatively constant in the other manipulation (see below).  
295 The  $D_{Sr}$  varies among foraminiferal taxa, often resulting in higher values than that of  
296 *Ammonia sp.* (e.g. *M. vertebralis* 0.17, *A. lessonii* 0.29, *A. hemprichii* 0.32, *H. depressa* 0.27-  
297 0.33, *N. calcar* 0.35, values taken from (Dueñas-Bohórquez et al., 2011; Raitzsch et al., 2010;  
298 Raja et al., 2005). Despite this variability in  $D_{Sr}$ , all foraminiferal values are higher than  
299 inorganic  $D_{Sr}$  values in the absence of Mg (ranging from 0.02 to 0.14; Lorens, 1981; Nehrke  
300 et al., 2007; Tesoriero and Pankow, 1996).

301 Field studies showed that partition coefficients ( $D_{Sr}$ ) range between 0.1-0.2 for *Uvigerina*  
302 spp., *Cibicidoides* spp., *Melonis barleeanum* and *Hoeglundina elegans* collected from core  
303 tops at various ocean basins (McCorkle et al., 1995; Elderfield et al., 1996; Rosenthal et al.,  
304 1997; Reichart et al., 2003; Lear et al., 2003; Yu et al., 2014). These studies noted an impact  
305 of pressure (Elderfield et al., 1996; Rosenthal et al., 1997) and preferential dissolution  
306 (McCorkle et al., 1995) on benthic foraminiferal Sr/Ca. In the field, temperature, salinity, pH  
307 and  $[CO_3^{2-}]$  do not have a noticeable impact on Sr/Ca (Yu et al., 2014) and the effect of  
308 pressure and post-mortem dissolution may be explained by the impact of  $\Delta[CO_3^{2-}]$  on Sr  
309 incorporation (Yu et al., 2014). These core-top series, however, do not allow to disentangle

310 impact of [DIC] versus  $\Delta[\text{CO}_3^{2-}]$  on foraminiferal Sr/Ca values since with increasing water  
311 depth, [DIC] generally increases, while saturation state decreases (Edmond and Gieskes,  
312 1970). In the field, Sr/Ca decreases with lower  $\Delta[\text{CO}_3^{2-}]$  (more corrosive conditions), which is  
313 parallel to an increase (our results) due to a higher [DIC]. These opposing effects of DIC and  
314  $\Delta[\text{CO}_3^{2-}]$  on foraminiferal Sr/Ca may dampen the so far reported effect of  $\Delta[\text{CO}_3^{2-}]$  on Sr  
315 incorporation from environmental samples.

316

#### 317 4.2. Correlation between foraminiferal Sr/Ca and C-system

318 Two different manipulations were used to alter seawater carbonate chemistry: TA  
319 manipulation (A1-A4) and pH-stable manipulation (B1-B4), while maintaining similar  
320 Sr/Ca<sub>sw</sub> across treatments (Table 1). The C-system parameters co-vary in both sets, but in a  
321 different way. As a result, certain parameters can be excluded as primary controls on  
322 observed changes in foraminiferal Sr/Ca. We can assume that if a certain C-system parameter  
323 is controlling incorporation of Sr into foraminiferal calcite, the correlation (i.e. trend or slope)  
324 between Sr/Ca and this parameter should be similar in both manipulations. Since this is not  
325 the case for  $p\text{CO}_2$  and carbonate ion concentration (Fig. 1c), these parameters do not exert the  
326 main controls on Sr/Ca in the species studied here.

327 In the case of pH, Sr/Ca values of the pH stable treatment exhibit a larger variability ( $\Delta$  in  
328 Sr/Ca of 0.8) when compared to the TA-manipulation treatment ( $\Delta$  is 0.2). If pH would have  
329 controlled Sr/Ca, the opposite should be true (constant Sr/Ca in the pH stable treatment and  
330 full range of variation in the TA manipulation). Since this is not the case (Fig. 1f), pH does  
331 not affect Sr-incorporation. This is also reflected in the results of the regression model (Table  
332 2): while  $p$  (the significance level of the test's outcome) and  $F$  (the ratio between the sample  
333 means variances and the variation within samples) remain statistically significant ( $p < 0.05$ ,  
334  $F = 12.43$ ), the  $R^2$  value is small (0.04) indicating that there is no predictive power of pH on  
335 foraminiferal Sr/Ca, as also indicated by the confidence intervals (Fig. S1). The conclusion  
336 that carbonate ion concentration and pH do not affect Sr/Ca in *Ammonia* is in accordance  
337 with one earlier study (Dueñas-Bohórquez et al., 2011), but in conflict with another (Dissard  
338 et al., 2010). This discrepancy might be explained by the experimental setup employed by  
339 Dissard et al. (2010), who changed salinity and temperature in addition to carbonate  
340 chemistry. Synergistic effects on calcification of, e.g., temperature and carbonate chemistry  
341 were reported for coccolithophores (Sett et al., 2014). Such synergistic effects might also be  
342 present in foraminifera, highlighting the importance of the experimental setup when  
343 comparing results from different studies. The observation that either carbonate ion  
344 concentration,  $\text{CO}_2$ , or pH affect Sr/Ca in e.g. *O. universa* (Russell et al., 2004) emphasizes  
345 the need to consider species-specific effects as has been shown for coccolithophores (Langer  
346 and Bode, 2011; Langer et al., 2006a).

347

348 Regarding the regression between Sr/Ca and bicarbonate ion concentration (Fig. 1b), it  
349 should be noted that the range in bicarbonate ion concentration is relatively small in the TA-  
350 manipulation (approximately 250  $\mu\text{mol/kg-sw}$ ), likely explaining the reduced significance of  
351 the regression ( $p = 0.02$ ) when compared to the pH-stable manipulation ( $p < 2e-16$ ). When  
352 taken at face value, the correlation of Sr/Ca and bicarbonate ion concentration in the TA-  
353 manipulation excludes bicarbonate ion concentration as a control on Sr/Ca. However, the  
354 small range in bicarbonate ion concentration in the TA-manipulation most likely renders this  
355 correlation meaningless. This conclusion is supported by the fact that all bicarbonate ion  
356 concentration values of the TA-manipulation fall on the regression line of the pH-stable-

357 manipulation (Fig 1b). Therefore, bicarbonate ion concentration might control Sr/Ca. A  
358 similar argument applies to TA and DIC (Fig 1d, e). Please note that bicarbonate ion  
359 concentration is the major constituent of both TA and DIC (Tab. 1). Therefore, bicarbonate  
360 ion concentration might be instrumental in the Sr/Ca change, whereas TA and DIC might  
361 merely accidentally correlate with Sr/Ca. This possibility is explored in detail in the next  
362 section.

#### 364 4.3. Biomineralization insights

365 Why should Sr/Ca in *Ammonia* be influenced by bicarbonate ion concentration, TA and/ or  
366 DIC? Since the correlations between TA and DIC and Sr/Ca is positive, it might be  
367 hypothesized that growth rate is the mediating agent (see also Russell et al., 2004; Dissard et  
368 al., 2010). This is, however, unlikely since 1) carbonate ion concentration influences growth  
369 rate in *Ammonia* more than the other C-system parameters (Keul et al., 2013a) and 2) in the  
370 present data set no correlation was observed between foraminiferal Sr/Ca and growth rate ( $p >$   
371 0.05). One of the central parameters in this context is the super-saturation of the DBS fluid  
372 with respect to calcite, the so called omega (Fig. 3). The DBS omega is the main control on  
373 calcite precipitation rate (Nielsen, 1964). The latter is probably regulated and fine-tuned by  
374 the organism in order to exert the necessary control on morphogenesis, chamber- and whole-  
375 test-growth rate. The DBS omega will be determined by both the influx of Ca and of DIC.  
376 Please note that DBS pH is kept high during chamber formation, facilitating the conversion  
377 of CO<sub>2</sub> to bicarbonate and eventually carbonate ion (De Nooijer et al., 2009a; 2009b; 2014b  
378 Glas et al., 2012). In our experiment, we increased the seawater DIC/bicarbonate  
379 concentration beyond typical sea surface water levels, thereby substantially increasing the  
380 flux of DIC into the DBS. This flux might be mediated by both bicarbonate ion concentration  
381 via membrane transporters, and CO<sub>2</sub> via diffusion through the lipid bilayer (Fig. 4). At least  
382 the diffusion of CO<sub>2</sub> cannot be controlled by the organism due to the steep pH gradient  
383 between DBS and microenvironment (De Nooijer et al., 2009a; Bentov et al., 2009; Glas et  
384 al., 2012). This enhanced DIC influx may elevate the omega ( $\Omega_{\text{calcite}}$ ) at the DBS. We assume  
385 that foraminifera counteract this rise in omega by reducing the DBS Ca influx. This  
386 assumption is reasonable, because all eukaryotic cells have a sophisticated machinery to  
387 regulate Ca fluxes (Medvedev, 2005). Reduced Ca influx will affect the Sr/Ca ratio of the  
388 DBS and therewith the  $D_{\text{Sr}}$  in relation to DIC (Fig. 4).

389

390

#### 391 4.4. Mathematical Exploration

392 The transmembrane transport model can be applied to the transport pathway of divalent  
393 cations (e.g. Mg, Sr and Ca) to describe the trace element to Ca ratios in the tests of  
394 foraminifera as a function of the trace element to Ca ratio in seawater. Here we explore the  
395 impact of DIC on foraminiferal Sr/Ca. A significant fraction of the carbon needed for  
396 calcification is probably due to passive diffusion of CO<sub>2</sub> into the cell (the "cheapest" option).  
397 In addition to that, HCO<sub>3</sub><sup>-</sup> probably needs to be actively transported into the cell to sustain  
398 high calcification rates. Both CO<sub>2</sub> and HCO<sub>3</sub><sup>-</sup> enter the DBS, where they are converted to  
399 CO<sub>3</sub><sup>2-</sup>, due to the high pH inside the DBS (see Fig. 4). The transport pathway of DIC species  
400 is not included in the recently proposed transmembrane transport model (Nehrke et al., 2013),  
401 but due to oversaturation considerations also of importance for minor element partitioning.  
402 Here, we fill this gap by assuming a tight regulation of calcification rate by foraminifera  
403 which may explain the linear dependence of  $D_{\text{Sr}}$  on DIC.

404

405 The value of  $D_{Sr}$  can be calculated according equation (11) in Langer et al. 2006b.

406 In order to describe different ionic compositions in seawater and in the DBS fluid we replace  
407 the concentrations by activities. The activity of  $Ca^{2+}$  in a compartment x, denoted by  $\{Ca^{2+}\}_x$ ,

408 is related the  $Ca^{2+}$  concentration  $[Ca^{2+}]_x$  by the activity coefficient  $\gamma_x$ :  $\{Ca^{2+}\}_x = \gamma_x [Ca^{2+}]_x$ .

409 The activity coefficient for  $Ca^{2+}$  in seawater,  $\gamma_{SW}$ , is around 0.2. In the DBS, the activity  
410 coefficient  $\gamma_{DBS}$  is assumed to be regulated by the cell, and probably range from 0.2 to almost

411 1.0. In terms of activities equation (11) in Langer et al. 2006b is given by:

412

$$413 \quad D_{Sr} = D_{Sr}^0 \frac{\{Ca^{2+}\}_{SW}}{\{Ca^{2+}\}_{DBS}} = D_{Sr}^0 \frac{\gamma_{SW} [Ca^{2+}]_{SW}}{\gamma_{DBS} [Ca^{2+}]_{DBS}}, \quad (2)$$

414

415 where  $D_{Sr}^0$  is the equilibrium value of  $D_{Sr}$ ,  $[Ca^{2+}]_{SW}$  the calcium concentration in seawater,  
416 and  $[Ca^{2+}]_{DBS}$  the calcium concentration at the site of calcification.  $[Ca^{2+}]_{DBS}$  and the internal  
417 carbonate ion concentration  $[CO_3^{2-}]_{DBS}$  determine the level of supersaturation of the DBS  
418 fluid with respect to calcite:

419

$$420 \quad \Omega = \frac{\{Ca^{2+}\}_{DBS} \{CO_3^{2-}\}_{DBS}}{K_S} = \frac{[Ca^{2+}]_{DBS} [CO_3^{2-}]_{DBS}}{K_{Sp}^*}, \quad (3)$$

421

422 with the thermodynamic solubility constant,  $K_S$ , and the so-called stoichiometric seawater  
423 saturation product  $K_{Sp}^*$ . It is assumed that  $\Omega_{calcite}$  is actively controlled by the foraminifera  
424 (homeostasis) to regulate calcification rate during chamber formation.

425 As there is no evidence for the existence of  $CO_3^{2-}$  ion channels or pumps and the equilibration

426 between  $CO_3^{2-}$  and  $HCO_3^-$  is almost instantaneous,  $[CO_3^{2-}]_{DBS}$  can be described as a constant  
427 fraction  $f$  of the bicarbonate ion concentration in the DBS ( $[HCO_3^-]_{DBS}$ ; for a given pH):

428  $[CO_3^{2-}]_{DBS} = f[HCO_3^-]_{DBS}$ . For an internal pH of 9 (Bentov et al., 2009, de Nooijer et al.

429 2009) the value of  $f$  is 1.14. Then, we obtain from equations (2) and (3) an expression of  $D_{Sr}$

430 in terms of  $\Omega_{calcite}$  and  $[HCO_3^-]_{DBS}$ :

431

$$432 \quad D_{Sr} = D_{Sr}^0 \frac{\gamma_{SW}}{\gamma_{DBS}} \frac{[Ca^{2+}]_{SW} f [HCO_3^-]_{DBS}}{\Omega K_{Sp}^*}. \quad (4)$$

433

434 The value of  $[HCO_3^-]_{DBS}$  can be estimated using a simple balance equation for the flux of  
435 bicarbonate in/out of the DBS. For simplicity, we assume a constant influx of bicarbonate,

436  $HC_{inf}$ , which results from the conversion of  $CO_2$  (diffusing in passively) to  $HCO_3^-$  and,

437 depending on the rate of calcite precipitation, also an active  $HCO_3^-$  transport. We further

438 assume that foraminifera regulate both  $[CO_3^{2-}]_{DBS}$  and  $[Ca^{2+}]_{DBS}$  to control  $\Omega_{calcite}$  and thus the

439 rate of calcite precipitation,  $\sim(\Omega_{calcite} - 1)^n$ , at a favorable level. For this  $\Omega_{calcite}$ -homeostasis

440 bicarbonate influx and/or efflux via ion channels (with a rate  $\sim\Delta[HCO_3^-]$ ) may play a key role

441 in controlling  $[HCO_3^-]_{DBS}$  and therewith  $[CO_3^{2-}]_{DBS}$ . Within this model  $[HCO_3^-]_{DBS}$  is

442 described in terms of the simple differential equation

443

$$444 \quad \frac{d[HCO_3^-]_{DBS}}{dt} = k_1 ([HCO_3^-]_{SW} - [HCO_3^-]_{DBS}) - k_2 (\Omega - 1)^n + HC_{inf}, \quad (5)$$

445  
 446 which for the assumption that  $\Omega = \text{constant}$  has the steady state solution  
 447

$$448 \quad [HCO_3^-]_{DBS} = [HCO_3^-]_{SW} + \frac{HC_{inf} - k_2(\Omega - 1)^n}{k_1}. \quad (6)$$

449  
 450 We describe the concentration of bicarbonate in the seawater as a constant fraction  $g$  of  
 451 dissolved inorganic carbon, i.e.  $[HCO_3^-]_{SW} = g[DIC]$ . When all experimental carbonate  
 452 chemistry data are plotted in  $DIC - [HCO_3^-]$  space, a linear regression with a slope of 0.895  
 453 can be fitted.

454  
 455  
 456 Then, we obtain from the equations (4) and (6) the following linear equation for the DIC  
 457 dependence of  $D_{Sr}$ :

$$458 \quad D_{Sr} = m \cdot [DIC] + n, \quad (7)$$

460  
 461 with the slope

$$462 \quad m = D_{Sr}^0 \frac{\gamma_{SW}}{\gamma_{DBS}} \frac{[Ca^{2+}]_{SW} f g}{\Omega K_{Sp}^*} \quad (8)$$

464  
 465 and the intercept

$$466 \quad n = D_{Sr}^0 \frac{\gamma_{SW}}{\gamma_{DBS}} \frac{[Ca^{2+}]_{SW} f}{\Omega K_{Sp}^*} \left( \frac{HC_{inf} - k_2(\Omega - 1)^n}{k_1} \right). \quad (9)$$

468  
 469 We use the experimental slope  $m = 2 \cdot 10^{-5} \mu\text{mol}^{-1} \text{ l}$  to calculate  $\Omega$  from the internal pH.  
 470 Assuming a pH of 9 at the site of calcification (DBS) and solving equation 7 for  $\Omega$ , yields an  
 471  $\Omega$  range of 5.4 - 26.9 (when  $\gamma_{SW}/\gamma_{DBS} = 0.2 - 1.0$ ,  $S = 33$ ,  $T = 25$ ,  $D_{Sr}^0 = 0.021$ ,  $K_{Sp}^* = 10^{-6.4}$   
 472  $\text{mol}^2 \text{ kg}^{-2}$  and  $[Ca^{2+}]_{SW} = 10 \text{ mmol l}^{-1}$ ). This relative high  $\Omega$  is comparable to *in vivo* levels of  
 473  $\Omega$  occurring during shell formation of an oyster. For this organism the  $\Omega$  value in the  
 474 extrapallial fluid (the medium of shell formation) was estimated to be in the range of about 16  
 475 to 27 (Sikes et al., 2000), indicating the feasibility of our model.

476  
 477 We want to stress, that the here proposed model is a mathematical exploration of the  
 478 observed dependency of  $D_{Sr}$  on seawater carbonate chemistry. In this model, the parameter of  
 479 the carbonate system, which is instrumental in altering  $D_{Sr}$  is DIC. Based on our experimental  
 480 results we identified either bicarbonate ion concentration, DIC or TA as the parameter  
 481 affecting  $D_{Sr}$ . Taken together, the experimental results and the model lead us to conclude that  
 482 bicarbonate ion concentration, DIC is the driving force behind the  $D_{Sr}$  change. This  
 483 conclusion is strongly supported when considering that TA cannot cause any changes in cell  
 484 physiology. The reason is that TA is a conceptual parameter, which is of great importance in  
 485 determining the C-system (Dickson, 1992) but has no “physical reality”, which could be  
 486 experienced by an organism.

487

488 The model proposed here is a continuation of a recent model for foraminiferal calcification  
489 (Nehrke et al., 2013). This model is based on the transmembrane transport of  $\text{Ca}^{2+}$  from  
490 seawater into the DBS and accidental uptake of other divalent cations and subsequent  
491 incorporation in the calcite crystal lattice. One way to test the model would be to measure  
492 other divalent cations, which are subjected to the same transport mechanism and should  
493 therefore display the same relationship to bicarbonate ion concentration or DIC. For instance,  
494 barium would be an ideal candidate, as it is physiologically inert as is Sr (Salisbury and Ross  
495 1992), which for instance excludes magnesium as a test candidate. Unfortunately, barium  
496 could not be measured in the setup used, as concentrations in the shell were too low. Similar  
497 experiments to the ones described here, maybe under elevated barium concentrations could  
498 be used to test the here-proposed model.

499

500

#### 501 4.5. Sr/Ca-DIC sensitivity and paleoceanographic implications

502 The here studied species, *A. aomoriensis*, is a shallow water benthic foraminifer and rarely  
503 used for palaeoceanographic reconstructions. However, it is ideally suited for our study,  
504 since it is adapted to an environment where carbonate chemistry frequently changes. This  
505 makes it likely that observed effects under experimental conditions as extreme as imposed  
506 here are not laboratory artefacts. The element composition (e.g. Mg/Ca and Sr/Ca) of  
507 *Ammonia* spp. is similar to that of many other rotalid species. Moreover, the dependency of  
508 element partitioning on environmental conditions (e.g. Mg incorporation as a function of  
509 temperature) is similar for many of these low-Mg perforate species (Wit et al., 2012;  
510 Toyofuku et al., 2011), which allows translation of our results to other benthic species. Inter-  
511 species differences in published calibrations, however, make it challenging to apply our  
512 results directly to genera other than *Ammonia* and derive accurate [DIC] reconstructions from  
513 benthic foraminiferal Sr/Ca values in general.

514

515 Despite this cautionary note, our described dependency of Sr/Ca to DIC may help explain  
516 reported inter-ocean differences in Sr/Ca of *Cibicidoides wuellerstorfi* (Yu et al., 2014).

517 Based on the average DIC concentrations in the deep Pacific and deep Atlantic, our  
518 calibration (Fig. 1) would predict a slightly larger difference in Sr/Ca than reported by Yu  
519 and co-workers. Such a mismatch in absolute Sr/Ca differences may, however, be caused by  
520 potential inter-species differences in Sr/Ca-DIC calibrations.

521 Stoll and Schrag (1998) have estimated that mean ocean Sr/Ca may change between 1 and 3  
522 % as a result of changing sea levels over glacial-interglacial cycles. Indeed, Martin and  
523 coworkers (2000) reported systematic downcore oscillations in foraminiferal Sr/Ca over these  
524 cycles, which were consistent between ocean basins, for both planktonic and benthic species.  
525 The amplitude in Sr/Ca change was 4-6% maximum and could not be correlated to  
526 dissolution or temperature effects. The authors discussed possible effects of salinity and pH,  
527 and although their attributed changes were too small (2% relative) to account for the full  
528 change, they pointed into the right direction of change. The authors therefore assigned the  
529 rest of the change to G-IG changes in mean ocean Sr/Ca.

530

531 Glacial-interglacial changes in carbonate chemistry are based on the well-documented  
532 increase in  $p\text{CO}_2$  during termination 1 from 180 to 280  $\mu\text{atm}$  (Petit et al., 1999) and a  
533 subsequent decrease in open ocean surface pH from 8.3 to 8.1 (Hönisch et al., 2009). Using

534 the software package CO2SYS (Pierrot et al., 2006), this increase in  $p\text{CO}_2$  resulted in an  
535 estimated increase in DIC of 130  $\mu\text{mol/kg}$ . Using our correlation between DIC and  
536 foraminiferal Sr/Ca (Fig. 1), this should have resulted in an increase in Sr/Ca<sub>cc</sub> of 1.2% (from  
537 1.268 to 1.284 mmol/mol). This change is, however, too small to account for the reported 2-  
538 4% change in foraminiferal Sr/Ca (Martin et al., 2000). Allen and coauthors (2016) have  
539 performed a similar DIC calibration study with the planktonic species *Globigerinoides*  
540 *sacculifer* and found a slope between Sr/Ca<sub>cc</sub> and DIC twice as steep as we found for *Ammonia*  
541 sp. Applying this linear regression equation would lead to a change in Sr/Ca<sub>cc</sub> between G and  
542 IG of approximately 3%, which is in the order of the reported average Sr/Ca<sub>cc</sub> changes over  
543 glacial-interglacial cycles (Martin et al., 2000). While the direction of the Sr/Ca-DIC  
544 calibration very likely is the same for different species (assuming similar biomineralization  
545 controls), the slope of the calibration may well vary between species (cf those for Mg/Ca and  
546 Temperature, see Regenberg et al., 2009 for an overview). This means that the absolute  
547 change in foraminiferal Sr/Ca as a response to the same environmental change will vary  
548 between species. Future development of foraminiferal Sr/Ca as a proxy for seawater DIC will  
549 have to show whether glacial-interglacial changes in carbonate chemistry can fully explain  
550 observed changes in planktonic foraminiferal Sr/Ca.

551 Different trace elemental calibrations have been proposed in the literature for several C-  
552 system parameters. This dataset is based on the same samples and analyses published in Keul  
553 et al. (2013b), where the dependence of U/Ca on carbonate ion concentration has been  
554 described. A major strength of trace elemental analyses via ICP-MS lies in the fact, that  
555 several elements can be analyzed simultaneously on the same single foraminiferal chamber.  
556 When combining Sr and U analyses on the same samples, the full C-chemistry can be  
557 calculated employing the regressions giving in this paper and in Keul et al (2013b). A  
558 combination with e.g. Mg/Ca and oxygen isotopes can allow for the calculation of  
559 temperature and salinity. In order to achieve these multi-proxy reconstructions, more  
560 culturing studies are needed to fully characterize the uncertainties associated. Multi-proxy  
561 reconstructions can then be used to correct for the mutual effects of trace elements and  
562 isotopes on each other.

563

## 564 5. Conclusions

565 In the field, potentially many environmental (i.e. target) parameters change in concert,  
566 making it rarely straight forward to isolate a single influence on a particular proxy. Therefore  
567 culture experiments provide a very useful approach: in the present study we not only  
568 identified seawater carbonate chemistry as an influence on Sr/Ca, but also narrowed the  
569 options down to bicarbonate ion concentration (DIC) in the benthic foraminifera *Ammonia*  
570 sp. Applying the DIC calibration to a published dataset of paleo-Sr/Ca supports the validity  
571 of Sr/Ca as a carbonate system proxy. Furthermore, our study also shows that more research  
572 is needed to fully understand the Sr-incorporation in deep sea species growing at different  
573 depths. We present a conceptual model that proposes how Sr is incorporated in foraminiferal  
574 calcification during biomineralization. Taking this model a step further and use it to explain  
575 multiple, environmental impacts on Sr/Ca requires both more experimental and field  
576 calibrations, as well as a more comprehensive understanding of foraminiferal  
577 biomineralization. For example, the ion transporters responsible for the influx of DIC  
578 (bicarbonate transporters, carbonate ion transporters, CO<sub>2</sub> diffusion) and Ca (seawater  
579 leakage, transmembrane transport) remain poorly understood.

580

581 Acknowledgements

582 We in particular wish to thank Klaus-Uwe Richter, Beate Müller and Ilsetraut Stölting for  
583 laboratory assistance. This research was funded by the Alfred Wegener Institute through  
584 Bioacid (Gerald Langer FKZ: 03F0608) and the European Community's Seventh Framework  
585 Programme under grant agreement 265103 (Gerald Langer, Project MedSeA). This work  
586 contributes to EPOCA “European Project on Ocean Acidification” under grant agreement  
587 211384. This work was funded in part by The European Research Council (ERC grant 2010-  
588 NEWLOG ADG-267931 HE) and the Natural Environment Research Council  
589 (NE/N011708/1). Nina Keul was the beneficiary of a doctoral grant from the AXA Research  
590 Fund while this study was conducted.

591

592

593 6. References

594

595 Allen, K.A., Hönisch, B., Eggins, S.M., Haynes, L.L., Rosenthal, Y. and Yu, J. (2016) Trace  
596 element proxies for surface ocean conditions: A synthesis of culture calibrations with planktic  
597 foraminifera. *Geochim. Cosmochim. Acta* 193, 197-221.

598 Bentov, S. and Erez, J. (2006) Impact of biomineralization processes on the Mg content of  
599 foraminiferal shells: A biological perspective. *Geochem. Geophys. Geosyst.* 7, Q01P08.

600 Berman, M.C. and King, S.B. (1990) Stoichiometries of calcium and strontium transport  
601 coupled to ATP and acetyl phosphate hydrolysis by skeletal sarcoplasmic reticulum.  
602 *Biochim. Biophys. Acta - Biomembr.* 1029, 235-240.

603 Bijma, J., Hönisch, B. and Zeebe, R.E. (2002) Impact of the ocean carbonate chemistry on  
604 living foraminiferal shell weight: Comment on 'Carbonate ion concentration in glacial-age  
605 deep waters of the Caribbean Sea' by W. S. Broecker and E. Clark. *Geochem. Geophys.  
606 Geosyst.* 3.

607 Bijma, J., Pörtner, H.-O., Yesson, C. and Rogers, A.D. (2013) Climate change and the oceans  
608 – What does the future hold? *Mar. Pollut. Bull.* 74, 495-505.

609 Boyle, E.A. (1988) Cadmium: Chemical tracer of deepwater paleoceanography.  
610 *Paleoceanogr.* 3, 471-489.

611 Broecker, W.S. and Clark, E. (2002) Carbonate ion concentration in glacial-age deep waters  
612 of the Caribbean Sea. *Geochem. Geophys. Geosyst.* 3, 1-14.

613 de Nooijer, L.J., Toyofuku, T., Oguri, K., Nomaki, H. and Kitazato, H. (2008) Intracellular  
614 pH distribution in foraminifera determined by the fluorescent probe HPTS. *Limnol.  
615 Oceanogr. Methods* 6, 610-618.

616 de Nooijer, L.J., Toyofuku, T. and Kitazato, H. (2009) Foraminifera promote calcification by  
617 elevating their intracellular pH. *Proc. Natl. Acad. Sci. U.S.A.* 106, 15374-15378.

618 de Nooijer, L.J., Hathorne, E.C., Reichart, G.J., Langer, G. and Bijma, J. (2014a) Variability  
619 in calcitic Mg/Ca and Sr/Ca ratios in clones of the benthic foraminifer *Ammonia tepida*. *Mar.  
620 Micropal.* 107, 32-43.

621 de Nooijer, L.J., Spero, H.J., Erez, J., Bijma, J. and Reichart, G.J. (2014b) Biomineralization  
622 in perforate foraminifera. *Earth-Sci. Rev.* 135, 48-58.

623 Delaney, M.L., W.H.Bé, A. and Boyle, E.A. (1985) Li, Sr, Mg, and Na in foraminiferal  
624 calcite shells from laboratory culture, sediment traps, and sediment cores. *Geochim.  
625 Cosmochim. Acta* 49, 1327-1341.

626 Dickson, A.G. and Millero, F.J. (1987) A comparison of the equilibrium constants for the  
627 dissociation of carbonic acid in seawater media. *Deep Sea Res. Part A. Oceanogr. Res. Pap.*  
628 34, 1733-1743.

- 629 Dickson, A.G. (1992) The development of the alkalinity concept in marine chemistry. *Mar.*  
630 *Chem.* 40, 49-63.
- 631 Dickson A. G., Sabine C. L. and Christian J. R. (2007) Guide to best practices for ocean CO<sub>2</sub>  
632 measurements. PICES Special Publication 3, 1-191.
- 633 Dissard, D., Nehrke, G., Reichart, G.J. and Bijma, J. (2010) Impact of seawater pCO<sub>2</sub> on  
634 calcification and Mg/Ca and Sr/Ca ratios in benthic foraminifera calcite: results from  
635 culturing experiments with *Ammonia tepida*. *Biogeosci.* 7, 81-93.
- 636 Dueñas-Bohórquez, A., da Rocha, R.E., Kuroyanagi, A., de Nooijer, L.J., Bijma, J. and  
637 Reichart, G.-J. (2009) Interindividual variability and ontogenetic effects on Mg and Sr  
638 incorporation in the planktonic foraminifer *Globigerinoides sacculifer*. *Geochim.*  
639 *Cosmochim. Acta* 75, 520-532.
- 640 Dueñas-Bohórquez, A., Raitzsch, M., de Nooijer, L.J. and Reichart, G.-J. (2011) Independent  
641 impacts of calcium and carbonate ion concentration on Mg and Sr incorporation in cultured  
642 benthic foraminifera. *Mar. Micropal.* 81, 122-130.
- 643 Edmond, J.M. and Gieskes, J.M.T.M. (1970) On the calculation of the degree of saturation of  
644 seawater with respect to calcium carbonate under in-situ conditions. *Geochim. Cosmochim.*  
645 *Acta* 3, 1261-1291.
- 646 Emiliani, C. (1955) Mineralogical and chemical composition of the tests of certain pelagic  
647 foraminifera. *Micropal.* 1, 377-380.
- 648 Erez, J. (2003) The source of Ions for Biomineralization in Foraminifera and their  
649 Implications for Paleooceanographic Proxies. *Rev. Mineral. Geochem.* 54, 115-149.
- 650 Glas, M.S., Langer, G. and Keul, N. (2012) Calcification acidifies the microenvironment of a  
651 benthic foraminifer (*Ammonia* sp.). *J. Exp. Mar. Biol. Ecol.* 424-425, 53-58.
- 652 Griffin, W.L., Powell, W.J., Pearson, N.J. and O'Reilly, S.Y., 2008, Glitter: Data reduction  
653 software for laser ablation ICP-MS; In Sylvester, P.J. (ed.), *Laser Ablation ICP-MS in the*  
654 *Earth Sciences: Current Practices and Outstanding Issues*, Mineralogical Association of  
655 Canada Short Course Series, Short Course 40, Vancouver, B.C., pp. 308-311.
- 656 Hayward, B.W., Holzmann, M., Grenfell, H.R., Pawlowski, J. and Triggs, C.M. (2004)  
657 Morphological distinction of molecular types in *Ammonia* - towards a taxonomic revision of  
658 the world's most commonly misidentified foraminifera. *Mar. Micropal.* 50, 237-271.
- 659 Hemming, N.G. and Hanson, G.N. (1992) Boron isotopic composition and concentration in  
660 modern marine carbonates. *Geochim. Cosmochim. Acta* 56, 537-543.
- 661 Hönisch, B., Hemming, N.G., Archer, D., Siddall, M. and McManus, J.F. (2009)  
662 Atmospheric Carbon Dioxide Concentration Across the Mid-Pleistocene Transition. *Science*  
663 324, 1551-1554.

- 664 Hönlisch, B., Ridgwell, A., Schmidt, D.N., Thomas, E., Gibbs, S.J., Sluijs, A., Zeebe, R.,  
665 Kump, L., Martindale, R.C., Greene, S.E., Kiessling, W., Ries, J., Zachos, J.C., Royer, D.L.,  
666 Barker, S., Marchitto, T.M., Moyer, R., Pelejero, C., Ziveri, P., Foster, G.L. and Williams, B.  
667 (2012) The Geological Record of Ocean Acidification. *Science* 335, 1058-1063.
- 668 Hoppe, C.J.M., Langer, G., Rokitta, S.D., Wolf-Gladrow, D.A. and Rost, B. (2012)  
669 Implications of observed inconsistencies in carbonate chemistry measurements for ocean  
670 acidification studies. *Biogeosci.* 9, 2401-2405.
- 671 Jochum, K.P., Weis, U., Stoll, B., Kuzmin, D., Yang, Q., Raczek, I., Jacob, D.E., Stracke, A.,  
672 Birbaum, K., Frick, D.A., Günther, D. andENZWEILER, J. (2011) Determination of Reference  
673 Values for NIST SRM 610–617 Glasses Following ISO Guidelines. *Geostand. Geoanal. Res.*  
674 35, 397-429.
- 675 Kaczmarek, K., Langer, G., Nehrke, G., Horn, I., Misra, S., Janse, M. and Bijma, J. (2015)  
676 Boron incorporation in the foraminifer *Ammonia lessonii* under a decoupled carbonate  
677 chemistry. *Biogeosci.* 12, 1753-1763.
- 678 Keul, N., Langer, G., de Nooijer, L.J. and Bijma, J. (2013a) Effect of ocean acidification on  
679 the benthic foraminifera *Ammonia* sp. is caused by a decrease in carbonate ion concentration.  
680 *Biogeosci.* 10, 6185-6198.
- 681 Keul, N., Langer, G., de Nooijer, L.J., Nehrke, G., Reichart, G.-J. and Bijma, J. (2013b)  
682 Incorporation of uranium in benthic foraminiferal calcite reflects seawater carbonate ion  
683 concentration. *Geochem. Geophys. Geosyst.* 14, 102-111.
- 684 Kiessling, W. and Simpson, C. (2011) On the potential for ocean acidification to be a general  
685 cause of ancient reef crises. *Glob. Chang. Biol.* 17, 56-67.
- 686 Kisakürek, B., Eisenhauer, A., Böhm, F., Garbe-Schönberg, D. and Erez, J. (2008) Controls  
687 on shell Mg/Ca and Sr/Ca in cultured planktonic foraminiferan, *Globigerinoides ruber*  
688 (white). *Earth Planet. Sci. Lett.* 273, 260-269.
- 689 Langer, G. and Bode, M. (2011) CO<sub>2</sub> mediation of adverse effects of seawater acidification  
690 in *Calcidiscus leptoporus*. *Geochem. Geophys. Geosyst.* 12, Q05001.
- 691 Langer, G., Nehrke, G., Probert, I., Ly, J., and Ziveri, P. (2009) Strain-specific responses of  
692 *Emiliana huxleyi* to changing seawater carbonate chemistry. *Biogeosci.* 6, 2637 - 2646.
- 693 Langer, G., Geisen, M., Baumann, K.-H., Kläs, J., Riebesell, U., Thoms, S. and Young, J.R.  
694 (2006a) Species-specific responses of calcifying algae to changing seawater carbonate  
695 chemistry. *Geochem. Geophys. Geosyst.* 7, Q09006.
- 696 Langer, G., Gussone, N., Nehrke, G., Riebesell, U., Eisenhauer, A., Kuhnert, H., Rost, B.,  
697 Trimborn, S. and Thoms, S. (2006b) Coccolith strontium to calcium ratios in *Emiliana*  
698 *huxleyi*: The dependence on seawater strontium and calcium concentrations. *Limnol.*  
699 *Oceanogr.* 51, 310-320.

700 Lea, D.W., Mashiotta, T.A. and Spero, H.J. (1999) Controls on magnesium and strontium  
701 uptake in planktonic foraminifera determined by live culturing. *Geochim. Cosmochim. Acta*  
702 63, 2369-2379.

703 Lorens, R.B. (1981) Sr, Cd, Mn and Co distribution coefficients in calcite as a function of  
704 calcite precipitation rate. *Geochim. Cosmochim. Acta* 45, 553-561.

705 Marchitto, T.M., Jr., Curry, W.B. and Oppo, D.W. (2000) Zinc Concentrations in Benthic  
706 Foraminifera Reflect Seawater Chemistry. *Paleoceanogr.* 15, 299-306.

707 Marchitto, T.M., Jr Oppo, D.W. and Curry, W.B., (2002) Paired benthic foraminiferal Cd/Ca  
708 and Zn/Ca evidence for a greatly increased presence of Southern Ocean Water in the glacial  
709 North Atlantic. *Paleoceanogr.* 17(3), 1038. doi:10.1029/2000PA000598.

710 Martin, P.A., Lea, D.W., Mashiotta, T.A., Papenfuss, T. and Sarnthein, M. (2000) Variation  
711 of foraminiferal Sr/Ca over Quaternary glacial-interglacial cycles: Evidence for changes in  
712 mean ocean Sr/Ca? *Geochem. Geophys. Geosys.* 1, 1004.

713 Medvedev, S.S. (2005) Calcium signaling system in plants. *Russ. J. Plant Physl.* 52, 249-270.

714 Mehrbach, C., Culberson, C.H., Hawley, J.E. and Pytkowicz, R.M. (1973) Measurement of  
715 the Apparent Dissociation Constants of Carbonic Acid in Seawater at Atmospheric Pressure.  
716 *Limnol. Oceanogr.* 18, 897-907.

717 Mewes, A., Langer, G., de Nooijer, L.J., Bijma, J. and Reichart, G.-J. (2014) Effect of  
718 different seawater Mg<sup>2+</sup> concentrations on calcification in two benthic foraminifers. *Mar.*  
719 *Micropal.* 113, 56-64.

720 Nehrke, G., Keul, N., Langer, G., de Nooijer, L.J., Bijma, J. and Meibom, A. (2013) A new  
721 model for biomineralization and trace-element signatures of foraminifera tests. *Biogeosci.* 10,  
722 6759-6767.

723 Nehrke, G., Reichart, G.J., Van Cappellen, P., Meile, C. and Bijma, J. (2007) Dependence of  
724 calcite growth rate and Sr partitioning on solution stoichiometry: Non-Kossel crystal growth.  
725 *Geochim. Cosmochim. Acta* 71, 2240-2249.

726 Nielsen, A.E. (1964) *Kinetics of Precipitation*. Pergamon Press.

727 Nürnberg, D., Bijma, J. and Hemleben, C. (1996) Assessing the reliability of magnesium in  
728 foraminiferal calcite as a proxy for water mass temperatures. *Geochim. Cosmochim. Acta* 60,  
729 803-814.

730 Pagani, M., Lemarchand, D., Spivack, A. and Gaillardet, J. (2005) A critical evaluation of the  
731 boron isotope-pH proxy: The accuracy of ancient ocean pH estimates. *Geochim. Cosmochim.*  
732 *Acta* 69, 953-961.

733 Petit, J.R., Jouzel, J., Raynaud, D., Barvov, N.I., Barnola, J.-M., et al. (1999) Climate and  
734 atmospheric history of the past 420,000 years from the Vostok ice core, Antarctica. *Nature*  
735 399, 429-436. doi:10.1038/20859.

- 736 Pierrot, D., Lewis, E. and Wallace, D.W.R. (2006) MS Excel program developed for CO<sub>2</sub>  
737 system calculations., in: ORNL/CDIAC-105. Carbon Dioxide Information Analysis Center,  
738 O.R.N.L. (Ed.). US Department of Energy, Oak Ridge, Tennessee (2006).
- 739 R Development Core Team (2012) R: A Language and Environment for Statistical  
740 Computing. R Foundation for Statistical Computing, Vienna, Austria. [http://www.R-](http://www.R-project.org)  
741 [project.org](http://www.R-project.org).
- 742 Raitzsch, M., Duenas-Bohorquez, A., Reichart, G.J., de Nooijer, L.J. and Bickert, T. (2010)  
743 Incorporation of Mg and Sr in calcite of cultured benthic foraminifera: impact of calcium  
744 concentration and associated calcite saturation state. *Biogeosci.* 7, 869-881.
- 745 Raitzsch, M., Kuhnert, H., Hathorne, E.C., Groeneveld, J. and Bickert, T. (2011) U/Ca in  
746 benthic foraminifers: A proxy for the deep-sea carbonate saturation. *Geochem. Geophys.*  
747 *Geosyst.* 12, Q06019.
- 748 Raja, R., Saraswati, P.K., Rogers, K. and Iwao, K. (2005) Magnesium and strontium  
749 compositions of recent symbiont-bearing benthic foraminifera. *Mar. Micropal.* 58, 31-44.
- 750 Regenberg, M., Steph, S., Nürnberg, D., Tiedemann, R., Garbe-Schönberg, D. (2009)  
751 Calibrating Mg/Ca ratios of multiple planktonic foraminiferal species with  $\delta^{18}\text{O}$ -calcification  
752 temperatures: Paleothermometry for the upper water column. *Earth Planet. Sci. Lett.* 278,  
753 324-336.
- 754 Reichart, G.-J., Jorissen, F., Anschutz, P. and Mason, P.R.D. (2003) Single foraminiferal test  
755 chemistry records the marine environment. *Geol.* 31, 355-358.
- 756 Rodríguez-Tovar, F.J., Uchman, A., Alegret, L. and Molina, E. (2011) Impact of the  
757 Paleocene–Eocene Thermal Maximum on the macrobenthic community: Ichnological record  
758 from the Zumaia section, northern Spain. *Mar. Geol.* 282, 178-187.
- 759 Röttger, R. (1973) Die Ektoplasimahülle von *Heterostegina depressa*  
760 (Foraminifera: Nummulitidae). *Mar. Biol.* 21, 127-138.
- 761 Russell, A.D., Hönisch, B., Spero, H.J. and Lea, D.W. (2004) Effects of seawater carbonate  
762 ion concentration and temperature on shell U, Mg, and Sr in cultured planktonic foraminifera.  
763 *Geochim. Cosmochim. Acta* 68, 4347-4361.
- 764 Salisbury and Ross 1992, *Plant Physiology*, Wadsworth Publishing Group, Co., Belmont,  
765 CA. 682 pp.
- 766 Sanyal, A., Hemming, N.G., Hanson, G.N. and Broecker, W.S. (1995) Evidence for a higher  
767 pH in the glacial ocean from boron isotopes in foraminifera. *Nature* 373, 234-236.
- 768 Sanyal, A., Bijma, J., Spero, H. and Lea, D.W. (1999) Empirical Relationship Between pH  
769 and the Boron Isotopic Composition of *Globigerinoides Sacculifer*: Implications for the  
770 Boron Isotope Paleo-pH Proxy. *Paleoceanogr.* 16.

- 771 Sanyal, A., Nugent, M., Reeder, R.J. and Bijma, J. (2000) Seawater pH control on the boron  
772 isotopic composition of calcite: evidence from inorganic calcite precipitation experiments.  
773 *Geochim. Cosmochim. Acta* 64, 1551-1555.
- 774 Sanyal, A., Bijma, J., Spero, H. and Lea, D.W. (2001) Empirical relationship between pH and  
775 the boron isotopic composition of *Globigerinoides sacculifer*: Implications for the boron  
776 isotope paleo-pH proxy. *Paleoceanogr.* 16, 515-519.
- 777 Sett, S., Bach, L.T., Schulz, K.G., Koch-Klavsen, S., Lebrato, M. and Riebesell, U. (2014)  
778 Temperature Modulates Coccolithophorid Sensitivity of Growth, Photosynthesis and  
779 Calcification to Increasing Seawater pCO<sub>2</sub>. *PLoS ONE* 9, e88308.
- 780 Sikes, C.S., Wheeler, A.P., Wierzbicki, A., Mount, A.S. and Dillaman, R.M. (2000)  
781 Nucleation and Growth of Calcite on Native Versus Pyrolyzed Oyster Shell Folia, *Biol. Bull.*  
782 198, 50-66.
- 783 Smith, A.D. and Roth, A.A. (1979) Effect of carbon dioxide concentration on calcification in  
784 the red coralline alga *Bossiella orbigniana*. *Mar. Biol.* 52, 217-225.
- 785 Spindler, M. and Röttger, R. (1973) Der kammerbauvorgang der großforaminifere  
786 *Heterostegina depressa* (Nummulitidae). *Mar. Biol.* 18, 146-159.
- 787 Stoll, H.M. and Schrag, D.P. (2000) Coccolith Sr/Ca as a new indicator of coccolithophorid  
788 calcification and growth rate. *Geochem., Geophys. Geosys.* 1, 1999GC000015.
- 789 Stoll, H.M. and Schrag, D.P. (2001) Sr/Ca variations in Cretaceous carbonates: relation to  
790 productivity and sea level changes. *Palaeogeogr. Palaeoclim. Palaeoecol.* 168, 311-336.
- 791 Tesoriero, A.J. and Pankow, J.F. (1996) Solid solution partitioning of Sr<sup>2+</sup>, Ba<sup>2+</sup>, and Cd<sup>2+</sup>  
792 to calcite. *Geochim. Cosmochim. Acta* 60, 1053-1063.
- 793 Van Achterbergh, E., Ryan, C.G., Jackson, S.E. and Griffin, W.L., 2001, Data reduction  
794 software for LA-ICP-MS: appendix; In Sylvester, P.J. (ed.), *Laser Ablation -ICP-Mass*  
795 *Spectrometry in the Earth Sciences: Principles and Applications*, Mineralogical Association  
796 of Canada Short Course Series, Ottawa, Ontario, Canada, v. 29, pp. 239-243.
- 797 Yu, J., Elderfield, H. and Hönisch, B. (2007) B/Ca in planktonic foraminifera as a proxy for  
798 surface seawater pH. *Paleoceanogr.* 22.
- 799 Yu, J., Foster, G.L., Elderfield, H., Broecker, W.S. and Clark, E. (2010) An evaluation of  
800 benthic foraminiferal B/Ca and δ<sup>11</sup>B for deep ocean carbonate ion and pH reconstructions.  
801 *Earth Planet. Sci. Lett.* 293, 114-120.
- 802 Zeebe, R.E. and Wolf-Gladrow, D.A. (2001) *CO<sub>2</sub> in Seawater: Equilibrium, Kinetics,*  
803 *Isotopes.* Elsevier Science B.V., Amsterdam.  
804  
805  
806

807 Figure captions

808

809 Figure 1: Foraminiferal Sr/Ca versus individual C-system parameters: a) pCO<sub>2</sub>, b)  
810 bicarbonate ion concentration, c) carbonate ion concentration, d) TA, e) DIC, and f) pH.  
811 Individual laser-ablation measurements are represented by x and +, whereas squares indicate  
812 mean values. Blue represents data from TA manipulation (A1-A4) and pink indicates pH-  
813 stable manipulation (B1-B4). Lines represent linear regression lines for Sr/Ca versus the  
814 respective C-system parameter for the TA- and pH-stable manipulation separately. Due to the  
815 relatively small range in x-axis variations in the correlation between Sr/Ca and DIC in the TA  
816 manipulation (blue, e), the significance of regression is confined and regression slope has  
817 been omitted.

818

819 Figure 2: Foraminiferal D<sub>Sr</sub> versus individual C-system parameters: a) pCO<sub>2</sub>, b) bicarbonate  
820 ion concentration, c) carbonate ion concentration, d) TA, e) DIC, and f) pH. Individual laser-  
821 ablation measurements are represented by x and +, whereas squares indicate mean values.  
822 Blue represents data from TA manipulation (A1-A4) and pink indicates pH-stable  
823 manipulation (B1-B4). Lines represent linear regression lines for Sr/Ca versus the respective  
824 C-system parameter for the TA- and pH-stable manipulation separately. Due to the relatively  
825 small range in x-axis variations in the correlation between Sr/Ca and DIC in the TA  
826 manipulation (blue, e), the significance of regression is confined and regression slope has  
827 been omitted.

828

829 Figure 3: Foraminiferal Sr/Ca versus Omega Individual laser-ablation measurements are  
830 represented by x and +, whereas squares indicate mean values. Blue represents data from TA  
831 manipulation (A1-A4) and pink indicates pH-stable manipulation (B1-B4). Lines represent  
832 linear regression lines for Sr/Ca versus the respective C-system parameter for the TA- and  
833 pH-stable manipulation separately.

834

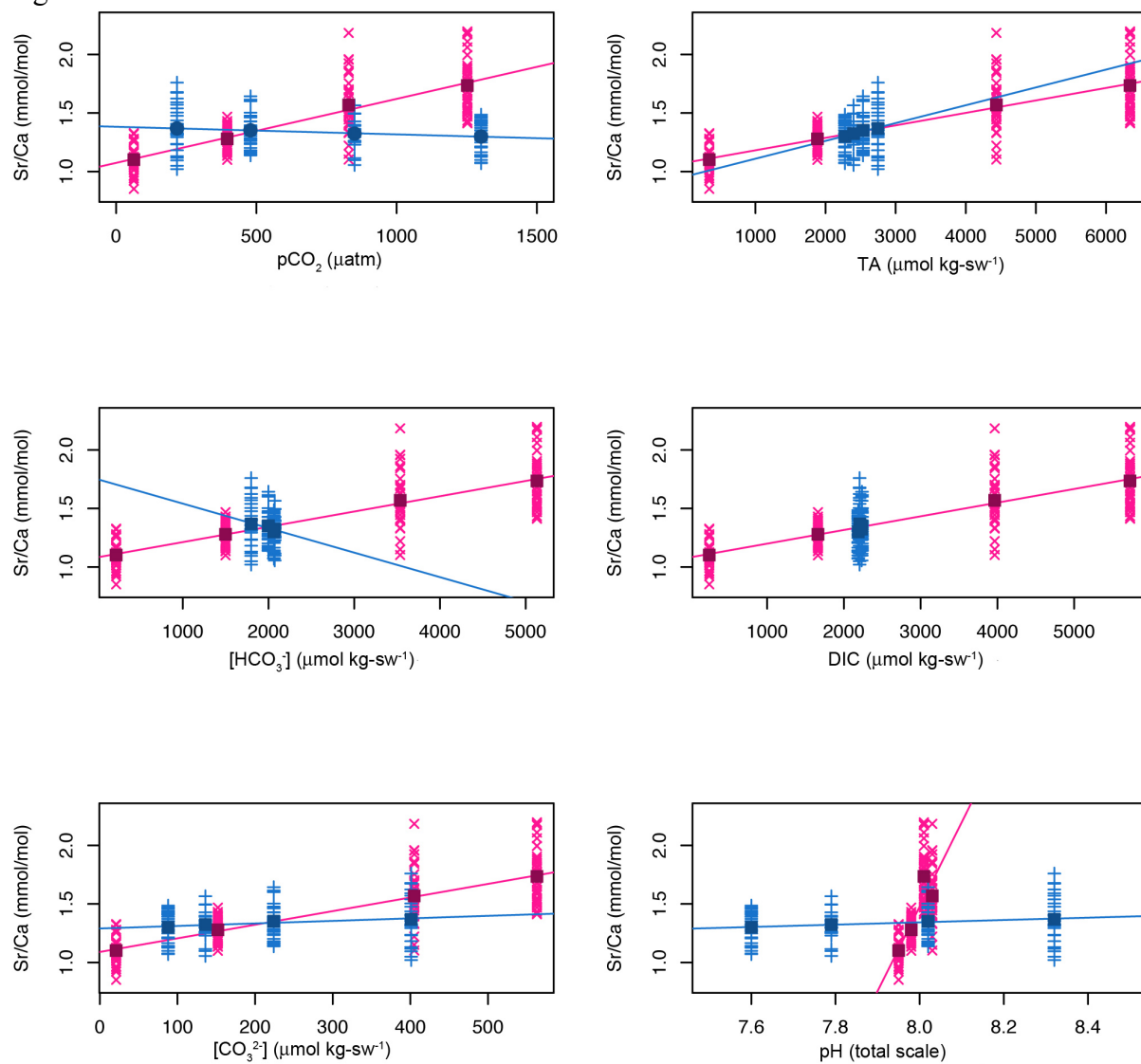
835 Figure 4: Schematic model of the processes during calcification. Calcite precipitation is  
836 thought to occur in a confined space ("delimited biomineralization space", DBS), which is  
837 created by the pseudopodial network (PN). Calcium carbonate (CC) is precipitated onto a  
838 template ("primary organic sheet", POS). A) The uptake of trace elements and its consequent  
839 incorporation into the calcite consists of two steps (inset in A): A1) Uptake from seawater  
840 into the DBS, where A2) the trace element is then incorporated into the calcium carbonate.  
841 During the uptake of Ca, small amounts of Sr also enter the DBS and consequently the CC.  
842 B1) High DIC in the culturing media leads to high CO<sub>2</sub> and HCO<sub>3</sub><sup>-</sup> concentrations. B2) Both  
843 of these enter the DBS, where they are converted to CO<sub>3</sub><sup>2-</sup>, due to the high pH inside the  
844 DBS. The red arrows depict this increase. B3) The foraminifera has to decrease Ca (red  
845 arrow) in order to keep  $\Psi$  constant. B4) The decrease of Ca inside the DBS causes Sr/Ca in  
846 the DBS to increase and consequently also in the calcite (red arrow), which is depicted  
847 graphically in B5).

848

849

850  
851

Figures  
Figure 1



852

Figure 2

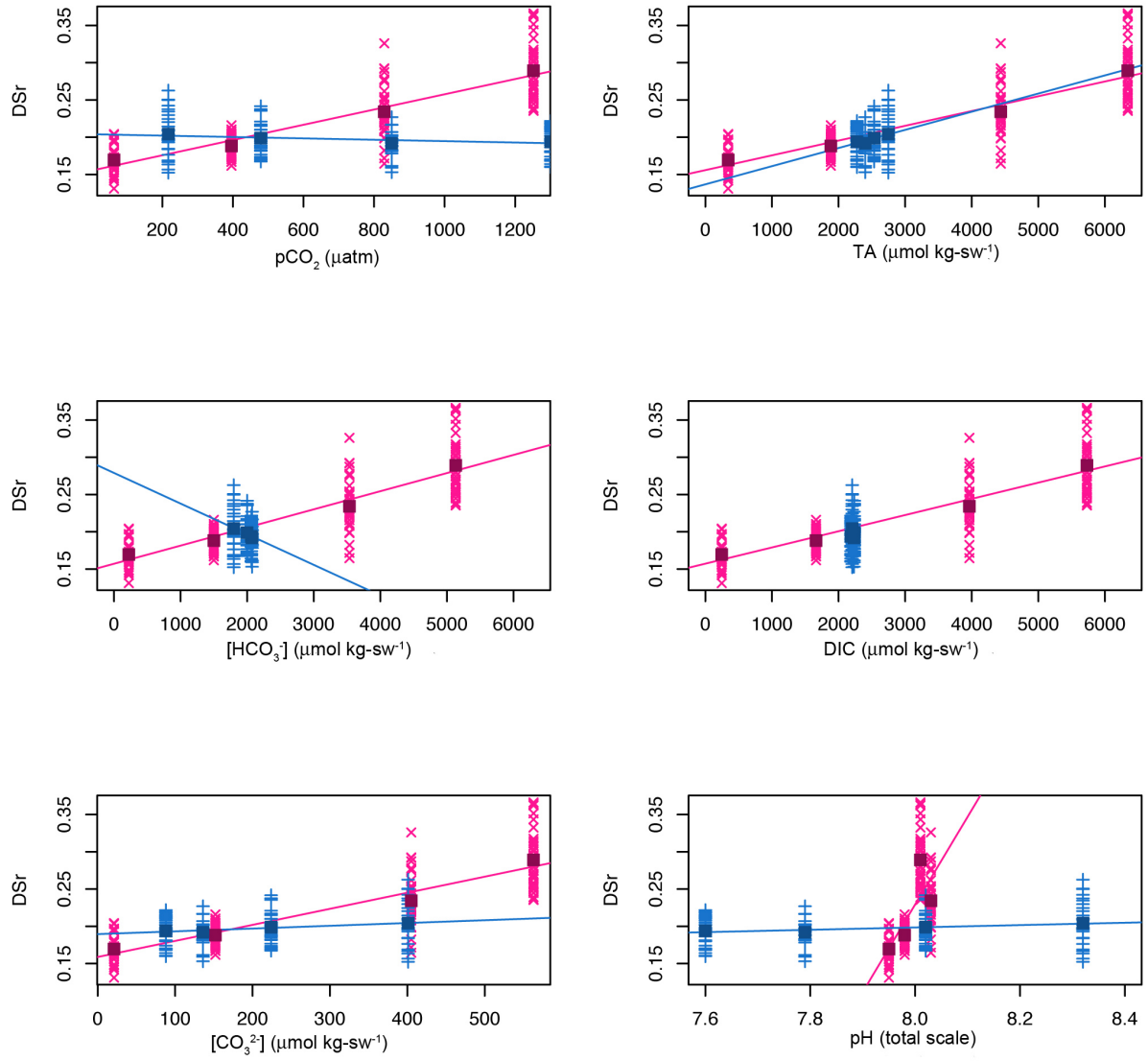
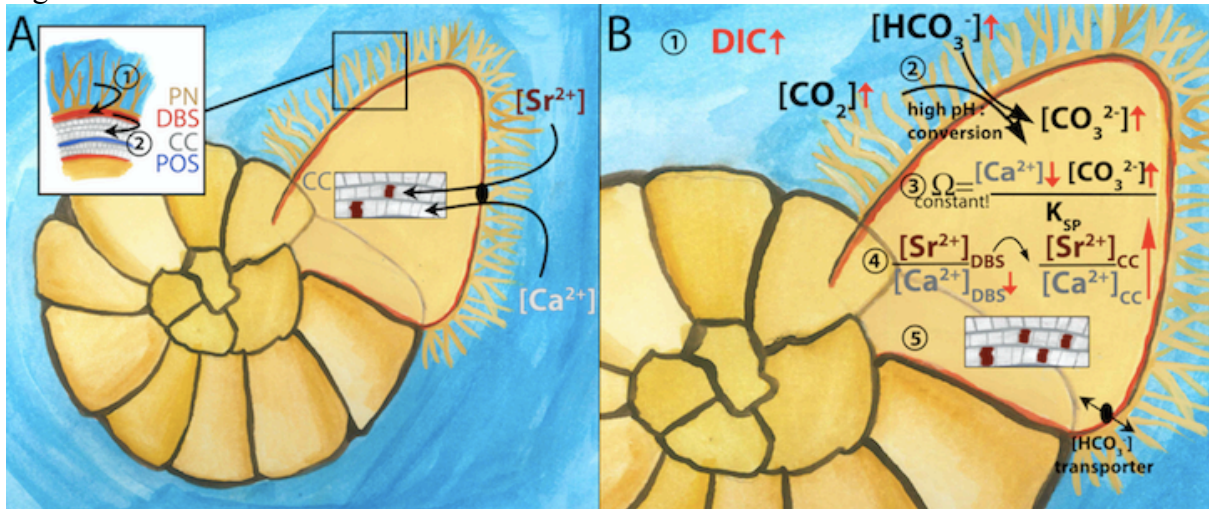


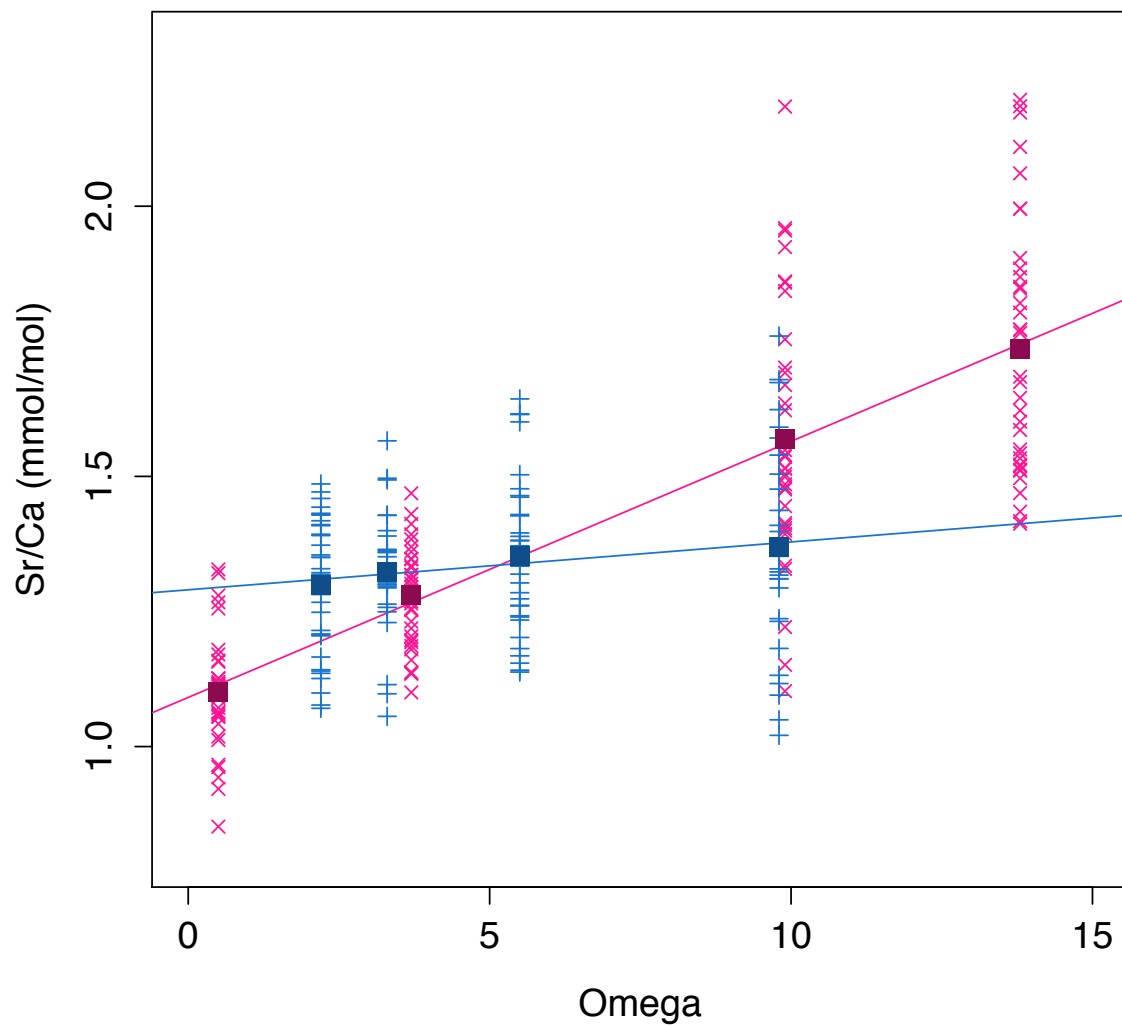
Figure 3



853  
854  
855

856

857 Figure 4



858

859 Table captions

860 Table 1: C-system parameters, Sr/Ca,  $D_{Sr}$  (calculated partition coefficient) and growth rates.  
861 DIC and pH of the seawater media were measured and used as input parameters to calculate  
862 the other C-system parameters using the CO2SYS software (Pierrot et al., 2006). Salinity and  
863 temperature were used as additional input parameters.  $pCO_2$  values supplied from the gas-  
864 mixing system are additionally listed ("nominal"). Stability was checked over the course of  
865 the experiment by regular pH measurements and control of the  $pCO_2$  provided by the gas-  
866 mixing system (precision approximately 10  $\mu atm$ ). Sr/Ca of the seawater media (sw) and  
867 calcite (cc) are listed as well as calculated partition coefficient  $D_{Sr}$  for TA manipulation (A1–  
868 A4) and pH-stable manipulation (B1–B4) treatments.  $\Omega_{cc} = [Ca^{2+}] * [CO_3^{2-}] / K_{sp}$  ( $K_{sp}$  =  
869 solubility constant).

870

871 Table 2: Linear regression analyses between foraminiferal Sr/Ca and respective C-system  
872 parameters. Listed is the intercept with the y-axis and the slope together with the associated  
873 standard errors (SE) for these parameters. Furthermore, p-value, F-value and  $R^2$  of the  
874 regression analyses are given.

875

Table 1

	Treatments							
	A1	A2	A3	A4	B1	B2	B3	B4
<b>pCO<sub>2</sub> (μatm)</b> "nominal"	180	380	950	1400	180	380	950	1400
<b>pCO<sub>2</sub> (μatm)</b>	217	479	850	1301	63	396	829	1252
<b>CO<sub>3</sub><sup>2-</sup> (μmol/kgSW)</b>	401	224	136	88	21	152	405	563
<b>HCO<sub>3</sub><sup>-</sup> (μmol/kgSW)</b>	1798	1999	2073	2063	223	1499	3536	5131
<b>DIC (μmol/kgSW)</b>	2205	2236	2232	2187	246	1662	3965	5729
<b>TA (μmol/kgSW)</b>	2747	2535	2400	2277	342	1884	4436	6343
<b>pH total scale</b>	8.32	8.02	7.79	7.60	7.95	7.98	8.03	8.01
<b>Ω<sub>cc</sub></b>	9.8	5.5	3.3	2.2	0.5	3.7	9.9	13.8
<b>Salinity</b>	32.8	32.8	32.8	32.8	32.7	32.7	32.8	32.6
<b>Sr/Ca sw (mmol/mol)</b>	6.7	6.8	6.9	6.7	6.5	6.8	6.7	6.0
<b>Sr/Ca cc (mmol/mol)</b>	1.4	1.4	1.3	1.3	1.1	1.3	1.6	1.7
<b>DSr</b>	0.20	0.20	0.19	0.19	0.17	0.19	0.23	0.29
<b>Growth rate (10<sup>-2</sup> μg/μm)</b>	11.2	7.3	7.6	9.7	6.0	9.3	12.8	9.0

Table 2

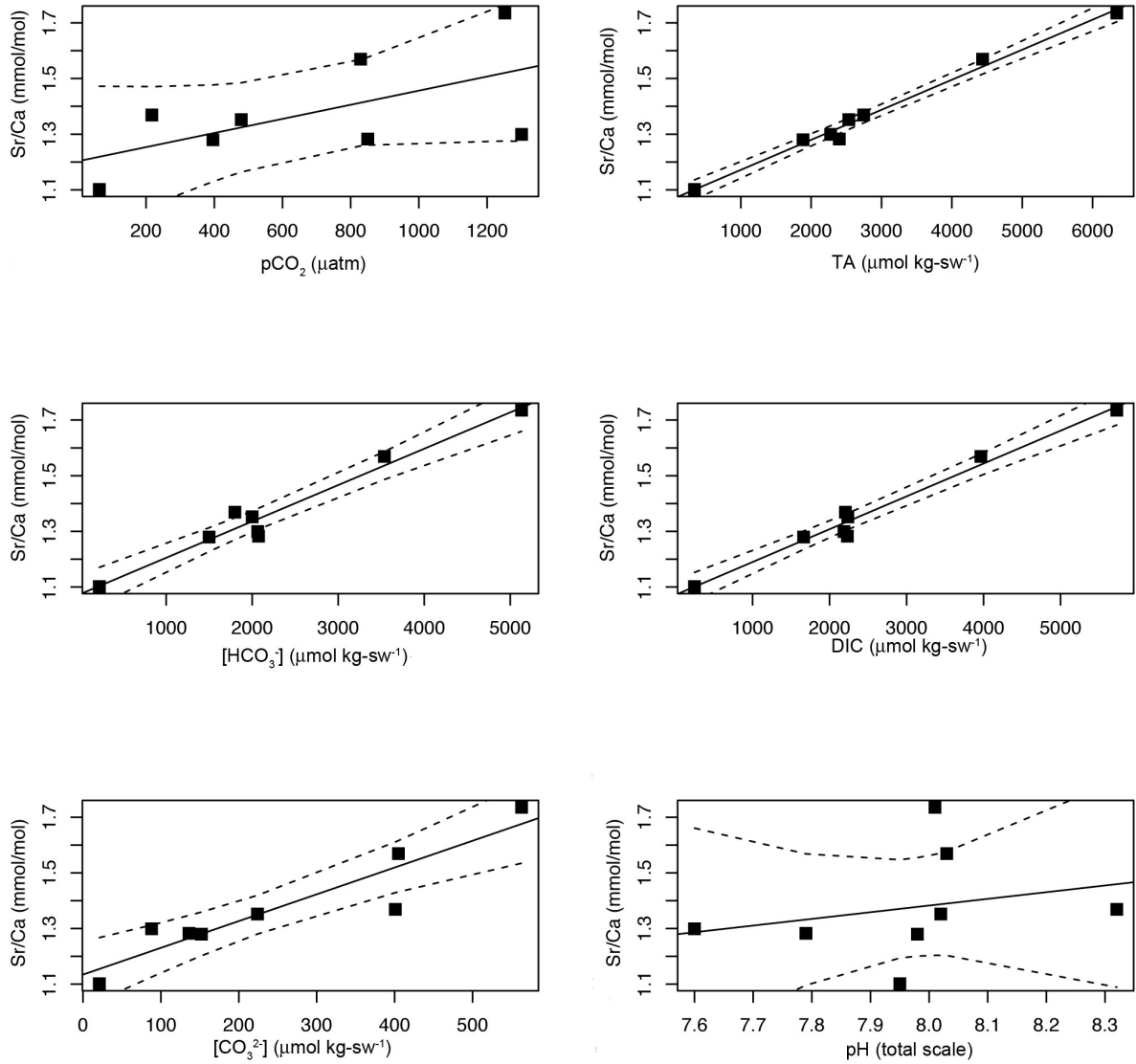
	all 8 treatments combined						
	Intercept	SE	slope	SE	p	R <sup>2</sup>	F
<b>pCO<sub>2</sub> (μatm)</b>	1.7E-01	4.4E-03	4.9E-05	5.4E-06	<2e-16	0.23	83.5
<b>CO<sub>3</sub><sup>2-</sup> (μmol/kgSW)</b>	1.6E-01	3.0E-03	1.9E-04	9.9E-06	<2e-16	0.56	355.5
<b>HCO<sub>3</sub><sup>-</sup> (μmol/kgSW)</b>	1.5E-01	3.1E-03	2.5E-05	1.2E-06	<2e-16	0.62	458.4
<b>DIC (μmol/kgSW)</b>	1.5E+00	3.1E-03	2.2E-05	1.0E-06	<2e-16	0.63	476.6
<b>TA (μmol/kgSW)</b>	1.5E-01	3.1E-03	2.1E-05	9.3E-07	<2e-16	0.64	490.8
<b>pH total scale</b>	-1.8E-01	1.1E-01	4.8E-02	1.4E-02	<0.001	0.04	12.4
<b>Ω<sub>cc</sub></b>	1.6E-01	3.0E-03	7.6E-03	4.0E-04	<2e-16	0.56	357.7

876

877

878  
879  
880

Supplementary Figures



S1: 95% Confidence Intervals for the regressions presented in Table 2.

881